Loss of *patched* and disruption of granule cell development in a pre-neoplastic stage of medulloblastoma

Trudy G. Oliver[1], Tracy Ann Read[1], Jessica D. Kessler[1], Anriada Mehmeti[1], Jonathan F. Wells[1], Trang T. T. Huynh[2], Simon M. Lin[3] and Robert J. Wechsler-Reya[1,*]

[1]Department of Pharmacology and Cancer Biology, Duke University Medical Center, Durham, NC 27710, USA
[2]Department of Radiation Oncology, Duke University Medical Center, Durham, NC 27710, USA
[3]Department of Biostatistics and Bioinformatics, Duke University Medical Center, Durham, NC 27710, USA
*Author for correspondence (e-mail: rw.reya@duke.edu)

Accepted 16 February 2005

Development 132, 2425-2439
Published by The Company of Biologists 2005
doi:10.1242/dev.01793

Summary

Medulloblastoma is the most common malignant brain tumor in children. It is thought to result from the transformation of granule cell precursors (GCPs) in the developing cerebellum, but little is known about the early stages of the disease. Here, we identify a pre-neoplastic stage of medulloblastoma in *patched* heterozygous mice, a model of the human disease. We show that pre-neoplastic cells are present in the majority of *patched* mutants, although only 16% of these mice develop tumors. Pre-neoplastic cells, like tumor cells, exhibit activation of the Sonic hedgehog pathway and constitutive proliferation. Importantly, they also lack expression of the wild-type *patched* allele, suggesting that loss of *patched* is an early event in tumorigenesis. Although pre-neoplastic cells resemble GCPs and tumor cells in many respects, they have a distinct molecular signature. Genes that mark the pre-neoplastic stage include regulators of migration, apoptosis and differentiation, processes crucial for normal development but previously unrecognized for their role in medulloblastoma. The identification and molecular characterization of pre-neoplastic cells provides insight into the early steps in medulloblastoma formation, and may yield important markers for early detection and therapy of this disease.

Key words: Medulloblastoma, Brain tumor, Pre-neoplastic, Patched, Hedgehog, Migration, Differentiation, Mouse

Introduction

Medulloblastoma is a highly malignant pediatric brain tumor (Zakhary et al., 2001). Despite significant improvements in treatment regimens, medulloblastoma remains one of the leading causes of cancer-related death in children under 9 years of age. A deeper understanding of the molecular basis of medulloblastoma is crucial for improving the early diagnosis and treatment of this devastating disease.

Approximately 25% of medulloblastoma cases have mutations in components of the Sonic hedgehog-Patched signaling pathway (Corcoran and Scott, 2001; Ellison et al., 2003). Sonic hedgehog (Shh) is a potent mitogen for cerebellar granule cell precursors (GCPs), the cells from which medulloblastoma is believed to arise (Wechsler-Reya and Scott, 2001; Wechsler-Reya and Scott, 1999). Patched functions as an antagonist of Sonic hedgehog signaling in most tissues (Ingham and McMahon, 2001). People with mutations in the *patched* gene develop Gorlin's syndrome, a disease characterized by basal cell carcinomas, skeletal defects and an increased incidence of medulloblastoma (Hahn et al., 1996; Johnson et al., 1996). Sporadic medulloblastomas also harbor mutations in *patched* and other elements of the Shh pathway (Lam et al., 1999; Raffel et al., 1997; Taylor et al., 2002). Finally, mice heterozygous for mutations in *patched* develop cerebellar tumors that resemble human medulloblastoma (Goodrich et al., 1997; Hahn et al., 2000).

Although *patched* mutant mice are an important model for medulloblastoma, the molecular and cellular basis of tumorigenesis in these mice remains unclear. Homozygous *patched* knockout mice die during embryonic development with defects in the nervous system, the heart and other tissues (Goodrich et al., 1997). Heterozygotes survive to adulthood, but after 3 months of age, 14-20% develop medulloblastoma (Goodrich et al., 1997; Wetmore et al., 2000). The status of the wild-type *patched* allele in these tumors is controversial: some studies have reported expression of wild-type *patched* in tumor tissue (Romer et al., 2004; Wetmore et al., 2000; Zurawel et al., 2000), whereas others have suggested that the wild-type allele is epigenetically silenced (Berman et al., 2002). Determining whether *patched* is lost – and when during tumorigenesis this loss occurs – is crucial for understanding the mechanisms of medulloblastoma formation.

Studies of *patched* mutant mice suggest that cerebellar abnormalities precede the appearance of tumors. While one-sixth of these animals develop medulloblastoma at 3-6 months of age, more than half have regions of ectopic cells in their cerebella at 4-6 weeks of age (Corcoran and Scott, 2001; Goodrich et al., 1997; Kim et al., 2003). These cells resemble normal GCPs in terms of morphology and location on the

surface of the cerebellum, and have therefore been described as remnants of the external germinal layer (EGL) from which GCPs originate. However, the presence of these cells in mice that are destined to develop medulloblastoma raises the possibility that they may represent a pre-neoplastic stage of tumorigenesis. Determining whether these cells are merely normal cells that persist into adulthood, or whether they are partially transformed cells on their way to becoming tumors has important implications for our understanding of granule cell development and tumorigenesis.

To gain insight into the early stages of medulloblastoma formation, we have isolated ectopic cerebellar cells from *patched* mutant mice and studied their molecular and functional characteristics. Our studies demonstrate that these cells share many properties with tumor cells: they express markers of the granule cell lineage, they exhibit activation of Shh target genes and they proliferate extensively in vitro. In addition, we show that these cells (and tumor cells) completely lack expression of the wild-type *patched* allele, suggesting a mechanism by which these cells maintain active hedgehog signaling. Finally, microarray analysis reveals that these cells have a unique pattern of gene expression that more closely resembles tumor cells than GCPs. Thus, it is likely these cells represent a distinct, pre-neoplastic stage of tumorigenesis. Genes that are differentially expressed at the pre-neoplastic stage include regulators of cell migration, survival and differentiation. Our studies suggest that loss of *patched* expression and dysregulation of these processes may be crucial early events in the development of medulloblastoma.

Materials and methods

Animals

Patched heterozygous mice (Goodrich et al., 1997) were obtained from Matthew Scott's laboratory at Stanford (CA, USA) and maintained by breeding with 129X1/SvJ mice from the Jackson Laboratories (Bar Harbor, ME). Math1-green fluorescent protein (Math1-GFP) transgenic mice (Lumpkin et al., 2003) were provided by Jane Johnson at UT Southwestern Medical Center (Texas, USA). Math1-GFP/*patched*$^{+/-}$ mice were generated by crossing *patched* heterozygotes with Math1-GFP mice, and then backcrossing to Math1-GFP mice three times before further analysis. All mice were maintained in the Cancer Center Isolation Facility at Duke University Medical Center.

Histological staining

To detect expression of β-galactosidase in intact cerebellum, tissue was isolated from adult wild-type or *patched*$^{+/-}$ mice (6- to 12-weeks old) and fixed in 4% paraformaldehyde (PFA) at 4°C. After fixation, tissues were permeabilized in buffer containing 0.01% deoxycholate and 0.02% IGEPAL CA-630 (both from Sigma, St Louis, MO, USA) for 10 minutes. Tissues were washed and stained overnight with X-gal reaction mixture containing 10 mM potassium ferrocyanide, 10 mM potassium ferricyanide, 0.4 mg/ml X-galactoside 5-bromo-4-chloro-3-indolyl-beta-D-galactopyranoside (X-gal, Sigma) in dimethyl sulfoxide, and 1 mM $MgCl_2$ in phosphate-buffered saline.

To compare expression of β-galactosidase and GFP in sections from Math1-GFP/*patched*$^{+/-}$ mice, cerebella were fixed in 4% PFA, cryoprotected in 25% sucrose, embedded in Tissue Tek-OCT (Sakura Finetek, Torrance, CA, USA) and cryosectioned sagittally at a thickness of 10 μm. One set of sections (for detection of GFP) was post-fixed for 10 minutes in 2% PFA and immediately mounted in Fluoromount G (Southern Biotechnology Associates, Birmingham, AL, USA). Adjacent sections were stained with X-gal as described above, counterstained with Nuclear Fast Red (Vector Laboratories, Burlingame, CA, USA) and mounted in Fluoromount G. Fluorescent (GFP) and bright-field (X-gal) images were acquired using a Nikon TE200 inverted fluorescent microscope and Openlab software (Improvision, Lexington, MA, USA).

For histochemical analysis of neonatal cerebellum, pre-neoplastic lesions and tumors, cerebella were fixed overnight in 10% formalin, transferred to 70% ethanol, paraffin wax-embedded and sectioned at 5 μm. Sections were stained with Hematoxylin and Eosin (Sigma).

Isolation of granule cell precursors, pre-neoplastic cells and tumor cells

Granule cell precursors (GCPs) were isolated from 7-day-old (P7) *patched*$^{+/-}$ mice; pre-neoplastic cells were obtained from 6-week-old *patched* mutants; and tumor cells were obtained from 10- to 25-week-old *patched* mutants displaying physical and behavioral signs of medulloblastoma. Cells were isolated from each source using a protocol described in (Wechsler-Reya and Scott, 1999). Briefly, cerebella were digested in solution containing 10 U/ml papain (Worthington, Lakewood, NJ, USA) and 250 U/ml DNase (Sigma), and triturated to obtain a cell suspension. This suspension was centrifuged through a step gradient of 35% and 65% Percoll (Amersham Biosciences, Piscataway, NJ, USA), and cells were harvested from the 35%-65% interface. Cells were resuspended in serum-free culture medium consisting of Neurobasal containing B27 supplement, sodium pyruvate, L-glutamine and penicillin/streptomycin (all from Invitrogen, Carlsbad, CA, USA), and counted on a hemacytometer. Cells used for RNA isolation were centrifuged and flash frozen in liquid nitrogen. For proliferation assays or immunostaining, cells were plated on poly-D-lysine (PDL)-coated tissue culture vessels and incubated in serum-free culture medium.

Flow cytometry and immunofluorescence

To detect β-galactosidase activity in isolated GCPs, pre-neoplastic cells and tumor cells, cells purified as described above were stained with fluorescein di-β-galactopyranoside (FDG, Marker Gene Technologies, Eugene, OR, USA) for 2 minutes at 37°C. Cells were washed, incubated for 30 minutes on ice and analyzed on a FACSVantage SE flow cytometer (BD Biosciences, San Jose, CA). As a control for non-specific FDG staining, GFP$^-$ cells were isolated by fluorescence-activated cell sorting (FACS) from Math1-GFP/*patched*$^{+/-}$ mice and stained in the same manner. These cells are not hedgehog responsive, and therefore express low levels of the mutant *patched* allele and low levels of β-galactosidase.

To detect expression of surface markers, cells were stained for 1 hour with primary antibodies, washed, stained for 30 minutes with secondary antibodies, and then analyzed by flow cytometry. To detect expression of intracellular markers, cells were plated (1 million cells/well) on PDL-coated coverslips in 24-well plates, and allowed to adhere for 4-6 hours before fixation with 4% PFA. Cells were stained overnight with primary antibodies, washed, stained with secondary antibodies for 2 hours at room temperature, and then mounted in Fluoromount G. Immunofluorescence was detected using a Nikon TE200 inverted microscope and Openlab software.

Antibodies used for flow cytometry and immunofluorescence included the following: nestin and GFAP (both from BD-Pharmingen, San Diego, CA, USA); O4, A2B5, polysialated (PSA)-NCAM and Zic-1 (all from Chemicon, Temecula, CA, USA); TUJ1 (Covance, Berkeley, CA, USA); and 13A4 anti-prominin/CD133 (a generous gift of Wieland Huttner and Denis Corbeil, Max Planck Institute, Dresden, Germany).

Proliferation assays

Cerebellar cells isolated as described above were resuspended in serum-free medium (Neurobasal + supplements) and transferred to PDL-coated 96-well plates, at a density of 2×10^5 cells/well. Cells

were pulsed immediately with tritiated thymidine (methyl-[^{3}H]-Td, Amersham, Arlington Heights, IL, USA) and cultured for 18 hours. Following culture, cells were harvested onto filters using a Mach IIIM Manual Harvester 96 (Tomtec, Hamden, CT, USA) and the amount of incorporated radioactivity was quantitated by liquid scintillation spectrophotometry using a Wallac MicroBeta microplate scintillation counter (Perkin Elmer, Boston, MA, USA).

RNA isolation and real-time RT-PCR

To isolate total cytoplasmic RNA from GCPs, pre-neoplastic cells and tumor cells, snap-frozen cell pellets were lysed in buffer containing 0.5% IGEPAL CA-630, digested with Proteinase K, extracted with phenol:chloroform:isoamyl alcohol, and precipitated with ethanol. RNA was purified using RNeasy columns (Qiagen, Valencia, CA, USA) and treated with DNase 1 (DNA-free, Ambion, Austin, TX, USA) to remove genomic DNA. RNA concentration was determined using the RiboGreen fluorescent dye (Molecular Probes, Eugene, OR, USA) with a TD-700 fluorometer (Turner BioSystems, Sunnyvale, CA, USA).

For real-time RT-PCR analysis, first-strand cDNA was synthesized using equivalent amounts of total RNA (0.1-1 μg) in a 20 μl reverse-transcriptase reaction mixture (Invitrogen). Real-time PCR reactions were performed in triplicate using a 25 μl mixture containing iQ SYBR Green Supermix (BioRad, Hercules, CA, USA), water, primers and 1 μl of cDNA. Gene-specific primers were used for: *Nmyc*, *cyclin D1*, *Gli1*, *Pax6*, *Unc5h3* (*Unc5c*), *Atf3*, *osteopontin* (*Spp1*), *Bag3*, *Foxf2*, *Klf4* and *Neurod1*; sequences for these are available upon request. Real-time quantitation was performed using the BIO-RAD iCycler iQ system (BioRad). Serial tenfold dilutions of cDNA were used as a reference for the standard curve calculation. Raw data were normalized based on expression of *actin*.

For analysis of wild-type and mutant *patched* expression, cells were isolated from Math1-GFP/*patched*$^{+/-}$ mice as described above, and then FACS-sorted to obtain pure populations of GFP$^+$ cells. RNA was isolated using the RNAqueous-Micro kit (Ambion), DNase-treated, quantitated, converted to cDNA and subjected to real-time PCR analysis as described above. Primers used to amplify *patched* were as follows: exons 2-3, 5′-GGC AAG TTT TTG GTT GTG GGT C-3′ (forward) and 5′-CCT CTT CTC CTA TCT TCT GAC GGG-3′ (reverse); and exons 7-9, 5′-CAT TGG CAG GAG GAG TTG ATT G-3′ (forward) and 5′-GCA CCT TTT GAG TGG AGT TTG G-3′ (reverse).

Microarray hybridization and analysis

RNA from GCPs, pre-neoplastic cells and tumor cells (isolated as described above, but not FACS-sorted), and from normal adult cerebellum (not dissociated), was converted to cDNA using the Superscript Choice cDNA kit (Invitrogen) and a T7-dT(24) primer (Genset/Proligo, Boulder, CO, USA). cRNA was generated using a T7-transcription/labeling kit from Enzo Life Sciences and hybridized to Affymetrix U74Av2 chips (Affymetrix, Santa Clara, CA, USA). Chips were scanned, and hybridization data were acquired using Affymetrix Suite 5.0 software. Affymetrix CEL files were normalized and quantified using Bioconductor software with the gcRMA model to quantify gene expression levels (Gentleman and Carey, 2002). Unsupervised principal components analysis (PCA) was used to identify the relationships among normal adult cerebellum, GCPs, pre-neoplastic cells and tumor cells based on expression profiles.

To identify genes that were differentially expressed among GCPs, pre-neoplastic cells and tumor cells, supervised analysis was carried out. A gene-by-gene analysis of variance (ANOVA) model with three groups (GCP, pre-neoplastic, tumor) was used to fit the $\log_2$-transformed intensities. To correct for multiple comparisons, the nominal *P*-value was adjusted using the false discovery rate (Benjamini and Hochberg, 1995). Genes were considered to be differentially expressed if they satisfied all of the following criteria: a difference in expression greater than 1.9-fold between any two groups; a maximum absolute intensity difference larger than 32 units; and an adjusted *P*-value <0.01. There were 118 genes that met these criteria. The identities of differentially expressed genes were verified by integrating data from the Affymetrix and Unigene databases. Gene functions were determined using information from Gene Ontology, Unigene, LocusLink and PubMed databases. Clustering was performed with Cluster and Treeview (Eisen et al., 1998). All statistical analysis was performed using R-1.7 software (Dalgaard, 2002). Results were visualized with Spotfire 6.0 (Somerville, MA, USA).

Immunohistological validation of microarray genes

Tissues were processed as described for the X-gal histological staining in the methods above for P7, 6-week-old, and 10- to 25-week-old *patched* mutant mice with tumors. PFA-fixed frozen sections were rehydrated in Tris-buffered saline and permeabilized with 2% Triton X-100 (Sigma) for 10 minutes. Sections were stained overnight at 4°C with rabbit polyclonal antibodies specific for Zic3 (Chemicon), Necdin (Upstate, Waltham, MA, USA) or Hsp105 (Biovision, Mountain View, CA, USA), or with mouse monoclonal antibodies specific for Pax6 (R&D Systems, Minneapolis, MN, USA). Antibody staining was detected using the EnVision+ Peroxidase-DAB system (Dako Cytomation, Carpinteria, CA, USA), as described in the manufacturer's protocol. Sections were counterstained with Harris Hematoxylin (Sigma) and mounted using Vectamount (Vector Laboratories).

Results

Detection of ectopic cerebellar cells in adult *patched* mutant mice

Patched mutant mice develop cerebellar tumors that resemble human medulloblastoma. These tumors are located on the surface of the cerebellum and express high levels of β-galactosidase (Fig. 1C). [When the *patched* mutant allele was generated, a portion of the *patched* gene was replaced with the β-galactosidase coding sequence (Goodrich et al., 1997); thus, staining with the β-galactosidase substrate X-gal reflects increased expression of the mutant *patched* allele.] Tumors occur in 15-20% of mice between 10 and 25 weeks of age. However, at 3-6 weeks of age, before any of the mice exhibit physical manifestations of tumor development, more than half have foci of ectopic β-galactosidase-expressing cells on the surface of their cerebellum (arrowheads in Fig. 1B). At early ages, several foci are commonly found in each animal; by 6-8 weeks, most animals have only one or two.

To examine the morphological characteristics of these cells, we sectioned cerebella from *patched* mutant animals and stained them with Hematoxylin and Eosin. At postnatal day 7 (P7), the cerebellum of *patched* mutant mice contains granule cell precursors (GCPs) on its surface and is indistinguishable from the cerebellum of wild-type mice (compare Fig. 2A with 2D). But by three weeks of age, wild-type and mutant cerebella are clearly different. In wild-type animals, all GCPs have differentiated and migrated inward, and the surface of the cerebellum consists mostly of neuronal processes (Fig. 2B,C). By contrast, 3-week-old *patched* mutant mice often have multiple regions of cells that have failed to migrate and instead remain on the surface of the cerebellum (Fig. 2E). These cells are densely packed and have a high nucleus:cytoplasm ratio (properties shared by both GCPs and tumor cells). In addition, staining with antibodies to the proliferation marker Ki67 reveals that a large percentage of these cells are in cycle (data not shown). Foci of ectopic cells are also seen in 6-week-old

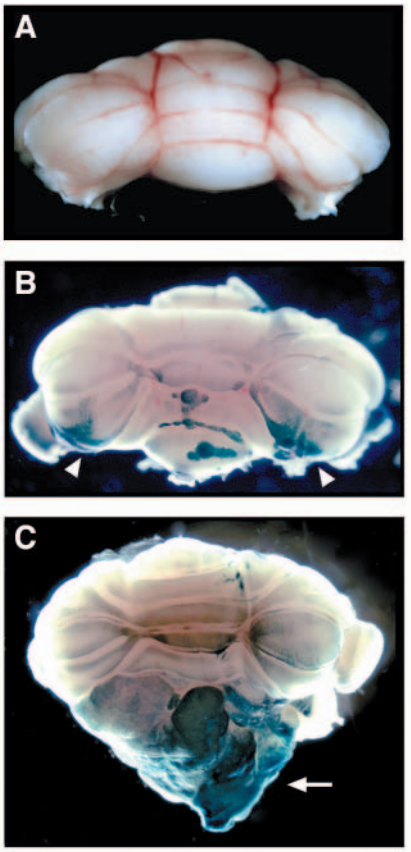

Fig. 1. The majority of *patched* mutant mice have ectopic cells in their cerebellum before they develop tumors. Cerebella from a 6-week-old wild-type mouse (A), a 6-week-old *patched*$^{+/-}$ mouse (B) and a 12-week-old *patched*$^{+/-}$ mouse with a tumor (C) were fixed and stained with X-gal. Tumors (arrow in C) are found in 15-20% of mutant mice between 10-25 weeks of age; these tumors express high levels of the mutant *patched* allele, which carries the β-galactosidase gene. At earlier ages, >50% of *patched* mutant mice have ectopic β-galactosidase-expressing cells (arrowheads in B). Background X-gal staining was not detected in the cerebellum of adult wild-type mice (A).

patched mutant animals (Fig. 2F), but are rarely observed beyond 10 weeks of age; at that age, *patched* mutant mice either show no cerebellar abnormalities or have large tumors that encompass the outer surface of their cerebellum (Fig. 2G). Thus, the majority of *patched* mutant mice have proliferating cells on the surface of their cerebellum well before they develop medulloblastoma.

The fact that the ectopic cells in *patched* mutants resemble tumor cells in terms of morphology, location and β-galactosidase expression – and occur in animals that are destined to develop tumors – suggests that they might represent an early, pre-neoplastic stage of medulloblastoma. Further studies of these cells (described below) strongly support this hypothesis; we therefore refer to them as 'pre-neoplastic cells' in the remainder of the text.

Pre-neoplastic cells express markers of immature granule cells

Previous studies have suggested that medulloblastoma arises from granule cell precursors (Buhren et al., 2000; Kadin et al., 1970; Miyata et al., 1998). To determine whether pre-neoplastic cells express markers of the granule cell lineage, we crossed *patched*$^{+/-}$ mice with Math1-GFP mice (Lumpkin et al., 2003). In the developing cerebellum, Math1 is a specific marker for proliferating granule cell precursors (Ben-Arie et al., 1996; Helms and Johnson, 1998). As GCPs cover the surface of the cerebellum during the first 2-3 weeks of life, the cerebellum of Math1-GFP mice is intensely fluorescent during this period (Fig. 3A). By 6 weeks of age, all GCPs have migrated inward and differentiated into mature granule neurons; thus, GFP is not expressed in the cerebellum of adult Math1-GFP mice (Fig. 3B). However, in Math1-GFP/*patched*$^{+/-}$ mice, regions of ectopic GFP^{+} cells are frequently seen in the cerebellum at 6 weeks of age (Fig. 3C,E). Tumors arising in these mice are also strongly GFP^{+} (Fig. 3D). These data suggest that pre-neoplastic cells and tumor cells express Math1 and are derived from the granule cell lineage.

To confirm that the GFP-expressing cells in adult Math1-GFP/*patched*$^{+/-}$ mice are the same as the ectopic β-galactosidase-expressing cells described above (Fig. 1), we sectioned cerebella from these mice and stained them with X-gal. As shown in Fig. 4A-C, GFP^{+} regions of cerebellum from 6-week-old mice show strong X-gal staining. Likewise, tumors from Math1-GFP/*patched*$^{+/-}$ mice show similar patterns of GFP expression and X-gal staining (Fig. 4D-F). Thus, in Math1-GFP/*patched*$^{+/-}$ mice, pre-neoplastic cells and tumor cells can be clearly identified by their expression of β-galactosidase and GFP. To gain insight into the early stages of tumorigenesis in *patched* mutant mice, we sought to isolate pre-neoplastic and tumor cells, and study their molecular and functional characteristics.

Isolation of pre-neoplastic cells and tumor cells from adult *patched* mutant mice

To isolate pre-neoplastic cells and tumor cells from *patched* mutant mice, we used a method originally developed for purifying neonatal GCPs (Oliver et al., 2003; Wechsler-Reya and Scott, 1999). This method selects for small, dense cells without processes, and destroys the majority of process-bearing neurons and glia that make up the normal adult cerebellum. Thus, when we used it to isolate cells from 6-week-old wild-type mice, we obtained an average of only 0.5 million cells per animal (n=10, range 0.2-0.9 million), and none of these cells had a morphology similar to that of GCPs. By contrast, when we performed this procedure on 6-week-old *patched* mutant mice, we obtained an average of 4.3 million GCP-like cells (n=43, range: 0.5-50 million) (Fig. 5A). Among *patched* mutant mice, 84% had more than 0.9 million cells, the highest number obtained from a wild-type mouse at this age. At 10-25 weeks of age, 16% of *patched* mutant mice had readily identifiable tumors. From these animals, we could isolate 50-600 million GCP-like cells (Fig. 5B). The remaining animals had no discernable abnormalities in their cerebellum, and we never obtained more than 2 million cells from them. These studies demonstrate that pre-neoplastic cells and tumor cells can be isolated from the cerebellum of *patched* mutant mice.

To verify that the cells we isolated from *patched* mutant mice represent the β-galactosidase-expressing cells identified by whole-mount staining of the cerebellum (Fig. 1), we stained

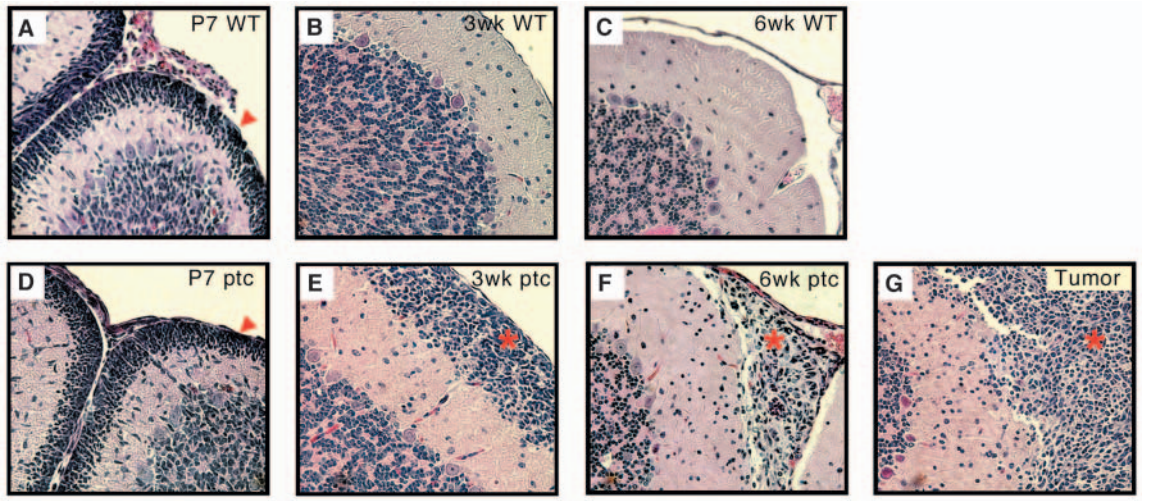

Fig. 2. Ectopic 'pre-neoplastic' cells resemble tumor cells. Cerebella were isolated from wild-type mice (A-C) and *patched*$^{+/-}$ mice (D-G) at 7 days (A,D), 3 weeks (B,E) 6 weeks (C,F) or 12 weeks (G) of age. Tissues were paraffin wax-embedded, sectioned and stained with Hematoxylin and Eosin. At 7 days of age, wild-type and *patched* mutant cerebella are indistinguishable, with densely-packed GCPs on the surface (arrowheads in A and D). Note the presence of ectopic cells on the outside of the cerebellum in adult *patched* mutant mice (asterisks in E and F) but not in wild-type mice (B,C). These cells are present in the majority of *patched* mutants, and resemble tumor cells (asterisk in G) in terms of size, morphology and location.

these cells with a fluorescent β-galactosidase substrate (FDG) and analyzed them by flow cytometry. As shown in Fig. 5C, the pre-neoplastic cells isolated from 6-week-old *patched* heterozygotes and tumor cells isolated from 16-week-old animals were 89-96% FDG^{+}. Moreover, when cells were isolated from Math1-GFP/*patched*$^{+/-}$ mice, 87% of pre-neoplastic cells and 95% of tumor cells were found to be GFP^{+}. Thus, freshly isolated pre-neoplastic cells and tumor cells, like their counterparts in situ, express high levels of β-galactosidase and Math1-GFP.

To further examine the phenotype of these cells, we isolated them and stained them with antibodies specific for various cell types (see Table S1 in supplementary material). Consistent with the expression of Math1-GFP, a large percentage of cells in each population expressed neuronal markers (tubulin βIII/TuJ1, polysialated NCAM and Zic1) (Miyata et al., 1998; Yokota et al., 1996). A small number of cells in each population expressed the oligodendrocyte marker O4 (Sommer and Schachner, 1981), suggesting that some cells of this lineage co-purify with GCPs in our isolation procedure. By contrast, very few cells expressed markers of astrocytes (glial fibrillary acidic protein) (Bignami et al., 1972) or neural stem cells (nestin, CD133/prominin) (Sawamoto et al., 2001; Weigmann et al., 1997). These findings support the notion that pre-neoplastic cells are derived from the granule cell lineage.

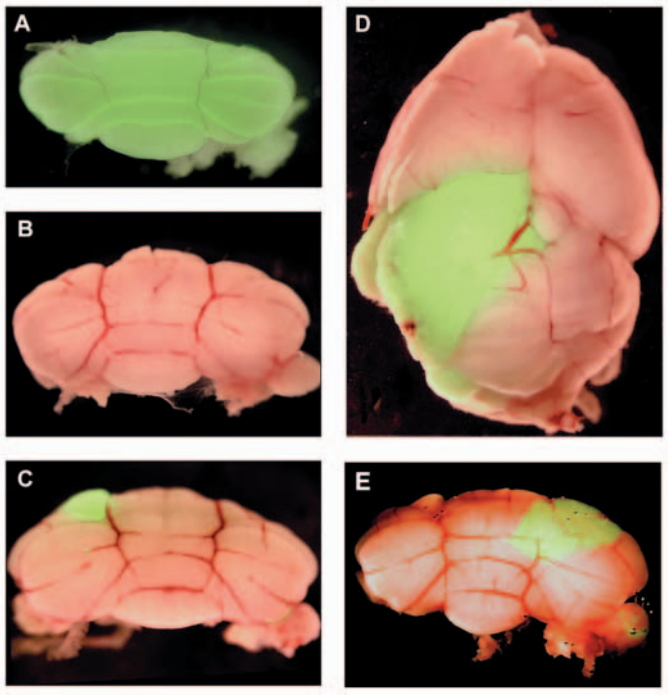

Fig. 3. Pre-neoplastic cells express the granule cell lineage marker Math1. Cerebella from 7-day-old (A) and 6-week-old (B) Math1-GFP transgenic mice, and from 6-week-old (C,E) and 18-week-old (D) Math1-GFP/*patched*$^{+/-}$ mice, were photographed using a Leica MZFLIII microscope equipped with SPOT camera and software. Fluorescent and bright-field images were overlaid using Photoshop. (D) Entire brain, with cerebellum (including tumor) at bottom. Note the GFP-expressing (green) pre-neoplastic and tumor regions (C-E) in *patched* mutant mice.

Pre-neoplastic cells express elevated levels of hedgehog target genes and proliferate in vitro

In *patched* heterozygotes, β-galactosidase activity is a reporter for expression of the mutant *patched* allele. Because *patched* is a target of the hedgehog pathway (Goodrich et al., 1996), the β-galactosidase activity observed in pre-neoplastic cells (Fig. 1B, Fig. 4C) suggests that these cells have increased activation of the hedgehog pathway. To determine whether these cells express elevated levels of other hedgehog target genes, we performed quantitative (real-time) RT-PCR analysis using primers specific for *Gli1*, *cyclin D1* and *Nmyc*, genes

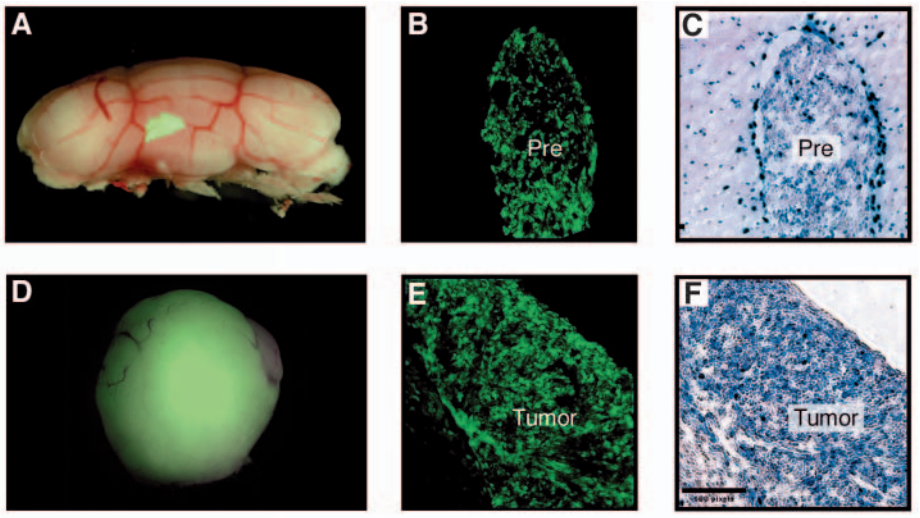

Fig. 4. Co-expression of Math1 and β-galactosidase in pre-neoplastic cells and tumor cells. Cerebella were isolated from 6-week-old (A-C) and 12-week-old (D-F) tumor bearing Math1-GFP/*patched*$^{+/-}$ mice. Intact cerebella (A,D) were photographed using a Leica MZFLIII microscope and then fixed, frozen and cryosectioned. One set of sections was mounted and photographed using a fluorescent microscope to detect GFP (B,E); adjacent sections were stained with X-gal, mounted and photographed under bright field (C,F). Note the correlation between GFP (green, indicative of Math1 expression) and X-gal staining (blue, indicative of mutant *patched* expression) in pre-neoplastic (B,C) and tumor-containing (E,F) regions.

previously identified as hedgehog targets in GCPs (Kenney et al., 2003; Kenney and Rowitch, 2000; Oliver et al., 2003; Wechsler-Reya and Scott, 1999). As a reference for the level of mRNA associated with hedgehog pathway activation, we compared the levels of these genes to the levels in resting granule cell precursors (cultured for 24 hours in the absence of Shh). As shown in Fig. 6, freshly isolated GCPs, pre-neoplastic cells and tumor cells all exhibit significantly elevated levels of Shh target genes when compared with resting cells (3- to 5-fold for *Nmyc*, 4- to 9-fold for *cyclin D1*, 2000- to 6000-fold for *gli1*). For each gene, the levels in GCPs, pre-neoplastic cells and tumor cells were comparable to or higher than the levels in cells that had been stimulated with Shh for 24 hours (data not shown). These data suggest that the Shh signaling pathway is activated in pre-neoplastic cells.

In granule cell precursors, Shh pathway activation is associated with proliferation (Kenney and Rowitch, 2000; Wechsler-Reya and Scott, 1999). To determine whether pre-neoplastic cells are proliferating, we measured thymidine incorporation in these cells following isolation. As shown in Fig. 6D, pre-neoplastic cells incorporate thymidine at levels comparable to freshly isolated GCPs and tumor cells. Thus, the pre-neoplastic stage is characterized by persistent hedgehog pathway activation and proliferation.

Pre-neoplastic cells lack expression of wild-type *patched*

Our studies indicated that GCPs, pre-neoplastic cells and tumor cells all exhibit hedgehog pathway activation and proliferation when they are isolated. In GCPs, expression of Shh targets reflects exposure to Shh in vivo prior to isolation (Kenney and Rowitch, 2000; Wechsler-Reya and Scott, 1999). In tumor cells, Shh pathway activation has been suggested to result from silencing of the wild-type *patched* allele (Berman et al., 2002), although some groups have reported persistent expression of wild-type *patched* in tumors (Romer et al., 2004; Wetmore et al., 2000; Zurawel et al., 2000). The status of wild-type *patched* in pre-neoplastic cells has not been investigated. Our ability to isolate pre-neoplastic cells and tumor cells to near-homogeneity allowed us to examine *patched* expression in these populations in the absence of contaminating (non-tumor) cells.

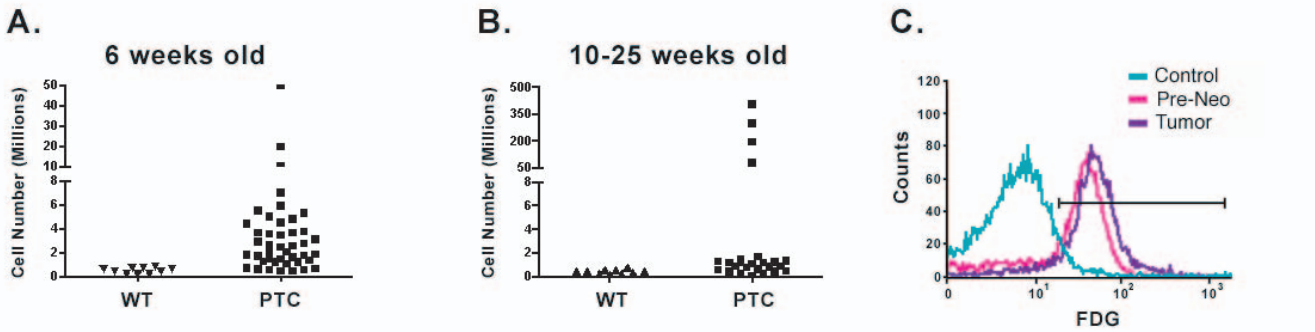

Fig. 5. Pre-neoplastic cells can be isolated from the cerebellum of *patched* mutant mice. Cells were isolated from the cerebellum of wild-type and *patched*$^{+/-}$ mice by enzymatic dissociation followed by Percoll gradient centrifugation, and viable cells were counted after Trypan Blue staining. (A) The average yield for 6-week-old wild-type mice was 0.53±0.25 million cells. For *patched* heterozygotes of the same age, the average yield was 4.3 million cells, with 84% of animals having more than 0.9 million cells (the maximum number seen in wild-type mice). (B) Among older *patched* mutants (10-25 weeks), 16% had tumors containing 50-600 million cells; the remainder had fewer than 2 million cells. (C) Non-granule cell precursors (GFP$^-$ cells from neonatal Math1-GFP/*patched*$^{+/-}$ mice), pre-neoplastic cells and tumor cells were stained with the fluorescent β-galactosidase substrate FDG and analyzed by flow cytometry. Relative fluorescence of non-GCPs (blue), pre-neoplastic cells (pink) and tumor cells (purple) is shown. The horizontal black line indicates the range of fluorescence considered to be positive (i.e. above background); 89% of pre-neoplastic cells and 96% of tumor cells exhibited fluorescence within this range.

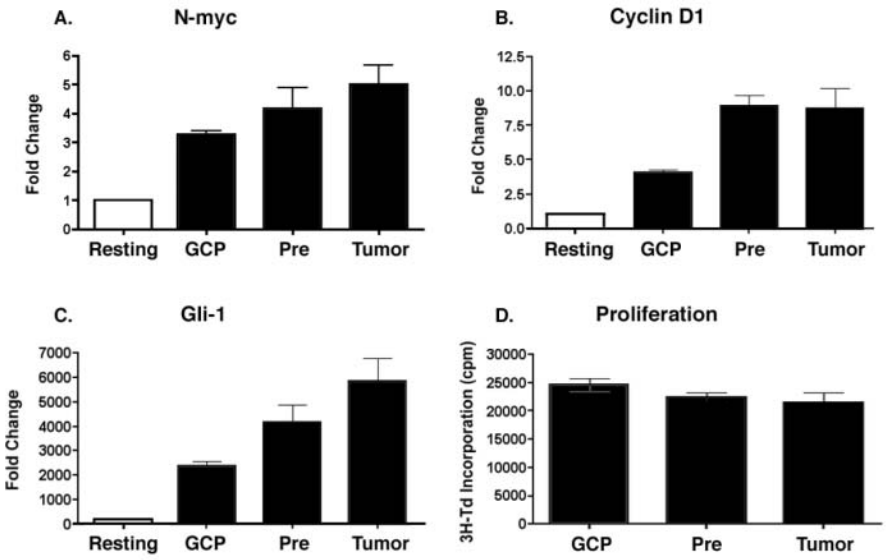

Fig. 6. Pre-neoplastic cells exhibit hedgehog pathway activation and proliferation. (A-C) Expression of hedgehog target genes. RNA was purified from freshly isolated GCPs, pre-neoplastic cells and tumor cells, and from GCPs cultured for 24 hours in the absence (resting) or presence (stimulated) of Sonic hedgehog (3 μg/ml Shh-N). Equivalent amounts of RNA were reverse transcribed and subjected to real-time PCR analysis using primers for *Nmyc* (A), *cyclin D1* (B) or *gli1* (C). Expression levels were normalized to *actin* and divided by the levels in resting GCPs to calculate fold induction. Data represent means of three samples of each cell type ±s.e.m. (D) Proliferation of GCPs, pre-neoplastic cells and tumor cells. Cells were pulsed with tritiated thymidine immediately after isolation, and then cultured for 18 hours in serum-free media before being harvested and assayed for thymidine incorporation. Data represent means of triplicate samples ±s.e.m., and are representative of 16 experiments.

We analyzed *patched* expression in GCPs, pre-neoplastic cells and tumor cells by real-time RT-PCR. To distinguish between wild-type and mutant *patched* transcripts, we used two sets of primers: one derived from exons 7-9, which are present in both the wild-type and mutant alleles, and another derived from exons 2-3, which can only amplify sequences present in the wild-type allele (see Fig. 7A). As shown in Fig. 7B, transcripts containing exons 7-9 were comparably expressed in GCPs, pre-neoplastic cells and tumor cells. By contrast, transcripts containing exons 2-3 (wild-type *patched*) were found in GCPs but were absent from the majority of pre-neoplastic cells and tumor cells (Fig. 7C). Similar results were seen using a pair of primers within exon 2. Overall, loss of wild-type *patched* was observed in 6 out of 7 pre-neoplastic samples and 13 out of 13 tumor samples, but was never seen in GCPs or in normal adult cerebellum from *patched*$^{+/-}$ mice (see Fig. S1 in supplementary material). These results suggest that the Shh pathway activation and proliferation seen in pre-neoplastic and tumor cells results from de-repression of the pathway due to loss of *patched*. Moreover, they indicate that loss of *patched* occurs at an early stage of tumorigenesis, well before cells have committed to becoming full-blown tumors.

Pre-neoplastic cells have a unique molecular signature

Together, the above data demonstrate that GCPs, pre-neoplastic cells and tumor cells are remarkably similar in terms of morphology, cell lineage, hedgehog pathway activation, and proliferation. However, all *patched* mutant mice have GCPs, whereas only a subset have detectable pre-neoplastic cells and only 16% develop tumors. Thus, despite their similarities, GCPs, pre-neoplastic cells and tumor cells must differ at a molecular level. To identify molecular differences between

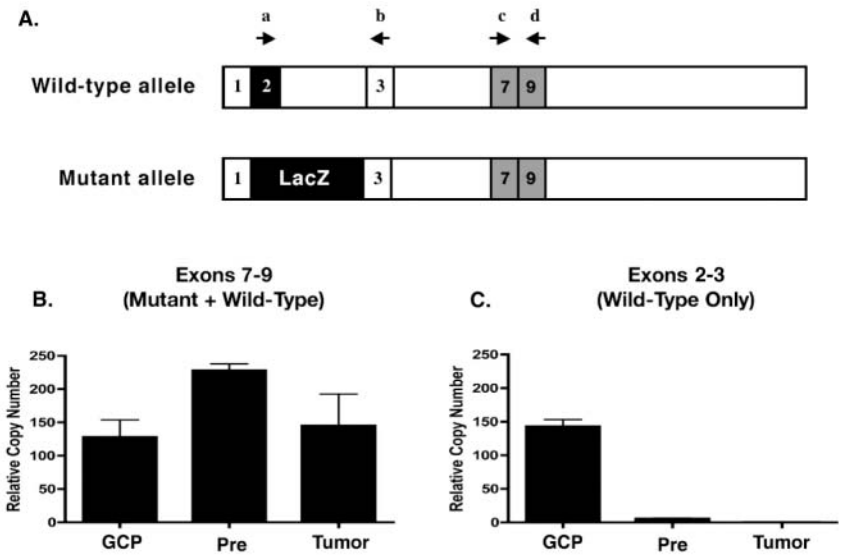

Fig. 7. Pre-neoplastic cells do not express wild-type *patched*. (A) Primers used to distinguish wild-type and mutant *patched* transcripts. The predicted structures of wild-type and mutant *patched* transcripts are shown. In the mutant allele, a portion of exon 1 and all of exon 2 have been replaced with the β-galactosidase coding sequence (*lacZ*). Thus, sequences within this region (detected by primers a and b) should only be present in wild-type transcripts. Sequences within exons 7 and 9 (detected by primers c and d) should be present in both wild-type and mutant transcripts. (B,C) Expression of wild-type and mutant *patched*. RNA from FACS-sorted GCPs, pre-neoplastic cells and tumor cells was subjected to real-time PCR analysis using primers c and d (exons 7-9, B) or primers a and b (exons 2-3, C). Expression levels were normalized to *actin*. Data represent means of three samples±s.e.m. Loss of wild-type *patched* expression was observed in six out of seven pre-neoplastic samples and 13 out of 13 tumor samples; see Fig. S1 in supplementary material for details.

GCPs, pre-neoplastic cells and tumor cells, we compared gene expression in these populations using DNA microarrays. RNA from GCPs, pre-neoplastic cells and tumor cells was labeled and hybridized to Affymetrix U74Av2 GeneChips, and data were analyzed using Bioconductor software (Gentleman and Carey, 2002) (see Materials and methods for details).

To determine how closely related these samples were in terms of gene expression, we performed unsupervised principal components analysis (PCA). When the analysis included normal adult cerebellum (Fig. 8A), GCPs, pre-neoplastic cells and tumor cells appeared highly similar to one another and quite distinct from adult cerebellum. This is not surprising, as adult cerebellum consists of postmitotic neurons and glia of various lineages whereas GCPs, pre-neoplastic cells and tumor cells are all proliferating cells derived from the granule cell lineage. By contrast, when GCPs, pre-neoplastic cells and tumor cells were compared directly to one another, each population exhibited a unique pattern of gene expression (Fig. 8B). Hierarchical clustering of the samples (Fig. 8C) supported this conclusion, and indicated that pre-neoplastic cells and tumor cells resemble one another more closely than either population resembles GCPs. Thus, GCPs, pre-neoplastic cells and tumor cells are readily distinguishable at a molecular level.

To characterize the differences in gene expression between GCPs, pre-neoplastic cells and tumor cells, we performed analysis of variance (ANOVA). This analysis identified 118 genes whose expression differed more than 1.9-fold (with a statistical confidence of $P<0.01$) between populations (see Fig. 9). Expression of 75 genes differed between GCPs and pre-neoplastic cells, and 80 genes distinguished GCPs from tumors. Only 34 genes changed between pre-neoplastic and tumor cells, consistent with the notion that these populations are more closely related to one another than to GCPs.

A large proportion of the differentially expressed genes were associated with three biological processes: cell migration, cell stress/apoptosis and differentiation (Table 1). Among the regulators of migration were extracellular matrix molecules (Osteopontin, Pleiotrophin, Procollagen IV), cell surface receptors (Unc5h3, Protein tyrosine phosphatase receptor type z) and transcription factors (Pax6). Genes associated with protection from cell stress included the transcription factor Atf3, the chaperone regulator Bag3, and several heat shock proteins. Finally, genes involved in cell fate and differentiation included transcription factors such as Foxf2, Klf4, Sox2, Neurod1 and Zic3. Significant differences in expression were also seen in genes encoding signaling molecules (G-protein coupled receptor 37-like 1, Gab1, Rhon, Calmodulin-like 4), metabolic genes (Carbonic anhydrase 2, Prostaglandin D2 synthase), channels (Aquaporin 4, Kcnd2), and secreted factors (Chemokine ligand 27, Vascular endothelial growth factor C). Finally, a number of sequences resembling endogenous retrovirus-like elements known as intracisternal A particles (IAPs) were found to be overexpressed at the tumor stage.

To confirm the results of our microarray analysis, we isolated RNA from independent samples of GCPs, pre-neoplastic cells and tumor cells and examined expression of representative genes using real-time RT-PCR. As shown in Fig. S2 (see supplementary material), each of these genes (Pax6, Unc5h3, Atf3, Osteopontin, Bag3, Foxf2, Klf4 and Neurod1) showed a distinct expression pattern in GCPs, pre-neoplastic cells and tumor cells, and the changes in expression were consistent with our microarray data. To test whether differentially expressed genes were targets of the Shh pathway, we cultured GCPs in the presence or absence of Shh protein for 12-24 hours and analyzed expression of select genes by real-time RT-PCR (data not shown). None of genes we tested were significantly altered by Shh stimulation, supporting the notion that the differences between GCPs, pre-neoplastic cells and tumor cells are not the result of differential Shh pathway activation. Finally, to determine whether the genes we identified in purified cells were also differentially expressed in situ, we used antibodies against the protein products of some of these genes to stain sections of neonatal (P7) cerebellum, pre-neoplastic lesions and tumors. As shown in Fig. 10, expression of these proteins (Zic3, Pax6, Necdin and Hsp105) was significantly different in GCPs, pre-neoplastic cells and tumor cells in situ, and mirrored the expression of the corresponding transcripts in purified cells.

Together these studies demonstrate that GCPs, pre-neoplastic cells and tumor cells can be distinguished at a molecular level and are likely to represent distinct stages of

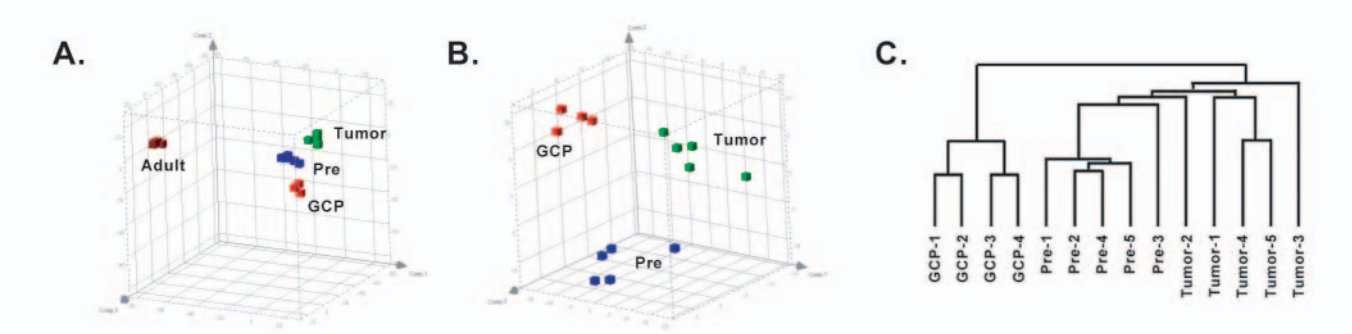

Fig. 8. GCPs, pre-neoplastic cells and tumor cells have distinct gene expression profiles. Gene expression in GCPs (four separate litters), pre-neoplastic cells (five mice), and tumor cells (five mice) from *patched* mutant mice, and adult cerebellum from wild-type mice (four mice), was analyzed using Affymetrix U74Av2 microarrays. Unsupervised principal components analysis (PCA) was used to assess the similarity in gene expression between these samples. (A) PCA plot of all 18 samples indicates that GCPs, pre-neoplastic cells and tumor cells are very similar to one another when compared with normal adult cerebellum. (B) Analysis excluding normal adult cerebellum suggests that compared with one another, GCPs, pre-neoplastic cells and tumor cells each have unique profiles of gene expression. (C) Single-linkage hierarchical clustering of the samples suggests that GCPs, pre-neoplastic cells and tumor cells are distinct, with pre-neoplastic and tumor cells resembling one another more closely than either resembles GCPs.

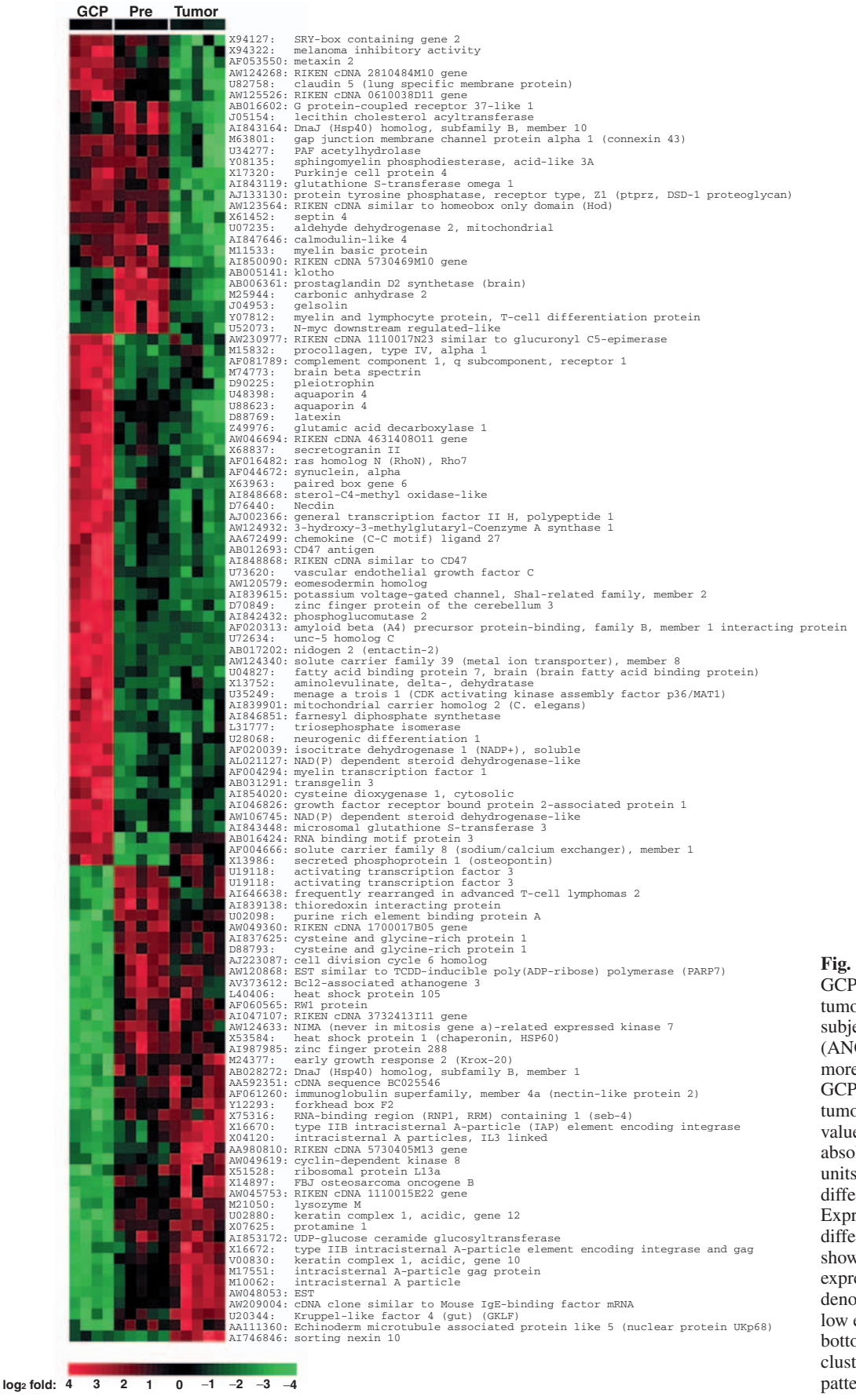

Fig. 9. Genes that distinguish GCPs, pre-neoplastic cells and tumor cells. Microarray data were subjected to analysis of variance (ANOVA) and genes that changed more than 1.9-fold between GCPs, pre-neoplastic cells and tumor cells (with adjusted *P*-values <0.01 and maximum absolute intensity difference >32 units) were considered differentially expressed. Expression profiles of the 118 differentially expressed genes are shown. Colors represent relative expression level, with red denoting high and green denoting low expression (see gradient at bottom of figure). Genes were clustered based on expression pattern among the three groups.

Table 1. Functions of differentially expressed genes

	Gene symbol	Unigene#	Type of molecule	Pre:GCP	Tumor:GCP
Adhesion/migration					
Secreted phosphoprotein 1 (osteopontin)	spp1, opn	Mm.257330	Extracellular matrix	–18.7	–2.5
Nidogen 2	nid2	Mm.20348	Extracellular matrix	–17.6	–22.1
Unc5 homolog C	unc5h3, unc5c	Mm.24430	Cell surface	–8.4	–9.3
Pleiotrophin	ptn	Mm.3063	Extracellular matrix	–4.4	–3.8
Collagen IV, alpha1	col4a1	Mm.738	Extracellular matrix	–3.8	–2.6
Paired box gene 6	pax6	Mm.3608	Transcription factor	–3.4	–4.7
CD47 (integrin-associated protein)	cd47, iap	Mm.167842	Cell surface	–2.5	–3.2
Protein tyrosine phosphatase, receptor type	ptprz1	Mm.41639	Cell surface	–1.6	–25.8
Gap junction protein a1 (Connexin 43)	gja1, cx43	Mm.4504	Cell surface	–1.4	–6
Platelet activating factor acetylhydrolase	pafah, pla2g7	Mm.9277	Secreted enzyme	–1.2	–5.7
Apoptosis/stress					
Bcl2-associated athanogene 3	bag3	Mm.28373	Chaperone regulator	9	4.1
Activating transcription factor 3	atf3	Mm.2706	Transcription factor	3.9	3
Heat shock protein 105	hsp105	Mm.270681	Chaperone	3.4	2.4
DnaJ (Hsp40) homolog B1	dnajb1	Mm.282092	Chaperone	2	2
DnaJ (Hsp40) homolog B10	dnajb10	Mm.248776	Chaperone	2	–2.5
Metaxin 2	mtx2	Mm.292613	Mitochondrial protein	–3.8	–29.4
Cell fate/differentiation					
FBJ osteosarcoma oncogene B	fosb	Mm.248335	Transcription factor	11.7	43
Forkhead box F2	foxF2	Mm.169989	Transcription factor	6.6	15.5
Kruppel-like factor 4	klf4, gklf	Mm.4325	Transcription factor	4.1	11.6
Cysteine and glycine-rich protein 1	csrp1	Mm.196484	Nuclear protein	3.8	2.9
Zinc finger protein 288	zfp288	Mm.211212	Transcription factor	3.5	2.7
Early growth response 2	egr2, krox20	Mm.290421	Transcription factor	2.7	3
Sry box containing gene 2	sox2	Mm.51994	Transcription factor	–1.7	–7.2
Neurogenic differentiation 1	neuroD1, beta2	Mm.4636	Transcription factor	–2.6	–2.4
Necdin	ndn	Mm.250919	Nuclear protein	–5	–8.6
Zinc finger protein of the cerebellum 3	zic3	Mm.4265	Transcription factor	–6.7	–11.1

Functions were assigned to genes based on information from Gene Ontology, Unigene, LocusLink and PubMed databases. Representative genes from the three major functional groups are presented. Numbers refer to the fold change in gene expression between GCPs and pre-neoplastic cells (Pre:GCP), and between GCPs and tumor cells (Tumor:GCP).

tumorigenesis. It is important to note that few of the genes that were differentially expressed between GCPs, pre-neoplastic cells and tumor cells were granule cell lineage markers, elements of the cell cycle machinery or known targets of the hedgehog pathway. This is consistent with our previous observation that these cells resemble one another in terms of lineage, hedgehog pathway activation and proliferation. By comparing similar populations of cells at different stages of tumorigenesis, we were able to identify other processes and pathways that contribute to medulloblastoma formation. The fact that pre-neoplastic cells and tumor cells have significant changes in genes that control migration, apoptosis and differentiation suggests that dysregulation of these processes may be crucial for the development of medulloblastoma.

Discussion

Medulloblastoma is a highly malignant and frequently fatal tumor, but little is known about the early stages of the disease. We have used a mouse model of medulloblastoma to identify a pre-neoplastic stage and define its molecular characteristics. Our data demonstrate that pre-neoplastic cells show elevated hedgehog pathway activation and proliferation, and lack expression of wild-type *patched*. In addition, pre-neoplastic cells have a unique molecular signature characterized by altered expression of genes that regulate migration, apoptosis and differentiation. These studies define a crucial early stage of tumorigenesis and provide insight into its molecular basis.

Pre-neoplastic cells in *patched* mutant mice were first described by Goodrich et al. as ‘regions of increased X-gal staining on the surface of the cerebellum’ (Goodrich et al., 1997). These cells have been suggested to represent either a persistent external germinal layer or an early stage of tumorigenesis (Corcoran and Scott, 2001; Goodrich et al., 1997; Kim et al., 2003). The distinction is important: if these cells are essentially normal GCPs (except for their persistence into adulthood), their relevance for understanding tumorigenesis may be limited. However, if they are partially transformed and need only acquire a small number of additional changes to become tumors, then studying their properties may shed light on the earliest changes required in medulloblastoma. Isolation of these cells has allowed us to study their molecular and functional characteristics in detail. Although pre-neoplastic cells resemble GCPs in terms of location, lineage and hedgehog pathway activation, they differ significantly from GCPs in terms of gene expression, including loss of *patched*. In these respects, pre-neoplastic cells are much more similar to tumor cells. Based on these observations, it is likely that they represent an early stage of tumorigenesis.

In this context, it is worth noting that persistent EGL has been observed in other mutant mice. For example, animals with mutations in brain-derived neurotrophic factor (BDNF), matrix metalloprotease 9 (MMP9), retinoid-related orphan receptor alpha (RORα/staggerer) or the peroxisome assembly gene PEX2 show delayed GCP migration and persistence of the EGL (Borghesani et al., 2002; Faust, 2003; Messer and Hatch,

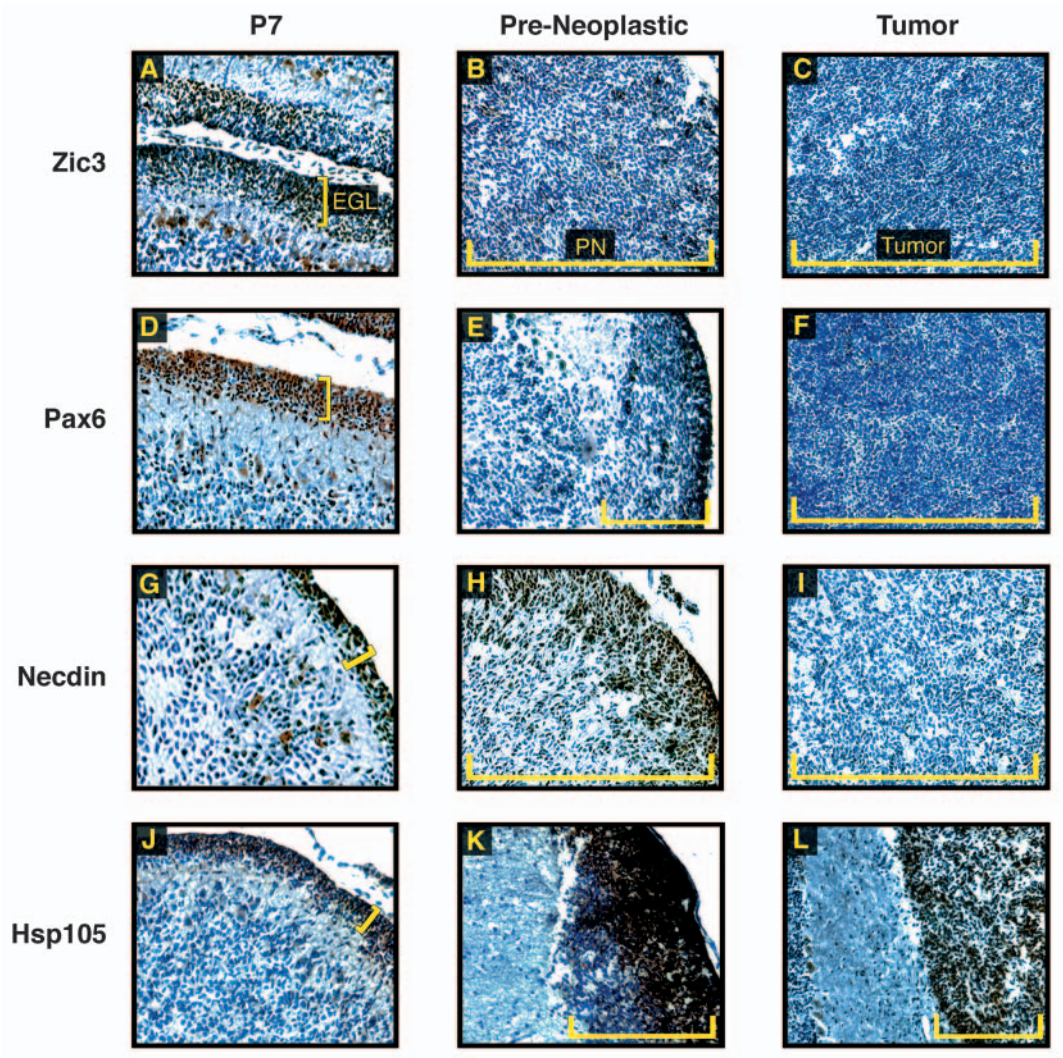

Fig. 10. Validation of microarray data by immunohistochemistry. Cryosections of neonatal (P7) cerebellum (A,D,G,J), pre-neoplastic lesions (B,E,H,K) and tumors (C,F,I,L) from *patched*$^{+/-}$ mice were stained with primary antibodies specific for Zic3 (A-C), Pax6 (D-F), Necdin (G-I) or Hsp105 (J-L) and peroxidase-conjugated secondary antibodies. Staining was detected using the peroxidase substrate DAB, which yields a dark brown precipitate. Yellow brackets mark the boundaries of the EGL (panels A,D,G,J), pre-neoplastic (PN) regions (B,E,H,K) and tumor (C,F,I,L). Expression of all four proteins is detectable in GCPs within the EGL. Consistent with microarray data, expression of Zic3 decreases significantly in pre-neoplastic lesions and is absent from tumors; Pax6 and Necdin are restricted to peripheral regions at the pre-neoplastic stage and are undetectable in tumors; and Hsp105 expression increases markedly at the pre-neoplastic stage and decreases somewhat in tumors.

1984; Vaillant et al., 2003). Moreover, astrotactin 1 null mice exhibit ectopic accumulations of GCPs that superficially resemble the foci observed in *patched* heterozygotes (Adams et al., 2002). However, none of these animals develop medulloblastoma, suggesting that persistence of the EGL alone is not sufficient for tumorigenesis. The fact that the ectopic cells in *patched* mutant mice more closely resemble tumor cells than GCPs – and occur in animals that develop tumors – supports the use of the term 'pre-neoplastic' to describe these cells.

Pre-neoplastic cells arise from proliferating granule cell precursors

The fact that pre-neoplastic cells and tumor cells express markers of the granule cell lineage is consistent with the notion that they are derived from granule cell precursors. The same has been postulated for human medulloblastomas, particularly those with a desmoplastic appearance (Buhren et al., 2000; Kadin et al., 1970; Miyata et al., 1998). Desmoplastic tumors – which represent 20-30% of human medulloblastomas – frequently harbor mutations in the Shh pathway, and have a gene expression profile that resembles normal GCPs (Pomeroy et al., 2002). Interestingly, recent studies have demonstrated that some human medulloblastomas (including desmoplastic tumors) express markers of neural stem cells (Hemmati et al., 2003; Singh et al., 2003; Singh et al., 2004). This could mean that they are derived from neural stem cells, or that they have acquired stem cell markers as a consequence of transformation (Oliver and Wechsler-Reya, 2004). Notably, few of the cells that we isolate from the *patched* mutant mice express markers of neural stem cells (nestin, CD133/prominin). Thus, tumorigenesis in the *patched* mutant mice does not appear to involve acquisition of a neural stem cell phenotype. Whether these cells exhibit other properties of neural stem cells – such as self-renewal or the capacity to differentiate into neurons and glia – remains to be determined.

Loss of *patched* and activation of the hedgehog pathway in pre-neoplastic cells

Our studies indicate that GCPs, pre-neoplastic cells and tumor cells express elevated levels of hedgehog target genes and proliferate in culture. In the case of GCPs, these responses probably reflect exposure to Shh in vivo shortly before isolation (Wechsler-Reya and Scott, 1999). In the case of pre-neoplastic cells and tumor cells, de-repression of the hedgehog pathway could result from loss of *patched* expression.

Although some studies have suggested that wild-type *patched* continues to be expressed in tumors (Romer et al., 2004; Wetmore et al., 2000; Zurawel et al., 2000), others have suggested that the wild-type *patched* locus in tumor cells may be silenced (Berman et al., 2002). Our studies support the latter view, demonstrating a striking loss of wild-type *patched* expression at both the pre-neoplastic and tumor stages.

One critical feature of our studies is the use of primers that distinguish between wild-type and mutant *patched* transcripts. In most studies that have reported continued *patched* expression in tumors from *patched* mutant mice, the data are based on northern analysis or in situ hybridization using probes that recognize both wild-type and mutant alleles. Although the mutant allele is clearly expressed in tumors, it is non-functional and would not be expected to contribute to the behavior of tumor cells. Our studies are also distinct in that we have separated pre-neoplastic and tumor cells from normal tissue. This is important because several cell types in the normal adult cerebellum express *patched* (Goodrich et al., 1997; Traiffort et al., 1999), and these cells can contribute significantly to RNA isolated from intact tumor tissue. By FACS-sorting cells that express Math1-GFP, we have eliminated these contaminating populations and analyzed expression of *patched* specifically in pre-neoplastic cells and tumor cells.

The mechanism by which *patched* is lost in pre-neoplastic cells and tumor cells remains unclear. Although studies of medulloblastoma cell lines derived from *patched*$^{+/-}$*p53*$^{-/-}$ mice have demonstrated that the wild-type *patched* allele can be silenced by methylation (Berman et al., 2002), we have found no evidence for this in primary tumor cells from *patched*$^{+/-}$ mice. Extensive sequencing of the four major CpG islands within and upstream of the *patched* promoter revealed no methylation in GCPs, pre-neoplastic cells or tumor cells (data not shown). Although methylation (or some other chromatin modification) could be present elsewhere in the *patched* gene, it is also possible that loss of *patched* expression results from mutations or deletions in the *patched* gene, or from loss of a signaling molecule or transcription factor that regulates *patched* expression. Mutational analysis of the *patched* locus, and studies of the transcription factors bound to the promoter, may help resolve this issue.

Regardless of the mechanism, our observation of decreased wild-type *patched* expression in both pre-neoplastic cells and tumor cells indicates that loss of *patched* is an early (and perhaps initiating) event in tumorigenesis. The fact that only a subset of pre-neoplastic cells develop into tumors implies that other changes besides loss of *patched* are required for the transition from the pre-neoplastic stage to more malignant stages of medulloblastoma. Whether these changes result from mutations or epigenetic events within pre-neoplastic cells themselves, or whether they arise from changes in the surrounding microenvironment, is an important question for future study.

Identification of genes associated with medulloblastoma progression

GCPs, pre-neoplastic cells and tumor cells resemble one another in many ways. And yet, GCPs are present in all of *patched* mutant mice (at the neonatal stage), pre-neoplastic cells are present in over half of these animals (at 6 weeks), and tumors occur in only 15-20%. Thus, these populations must differ from one another. To identify intrinsic differences between GCPs, pre-neoplastic cells and tumor cells, we analyzed gene expression using microarrays. These studies revealed that the three populations are remarkably similar when compared with normal adult cerebellum, but show significant differences when compared directly to one another. Notably, because all three populations exhibit hedgehog pathway activation and proliferation, differentially expressed genes include few hedgehog targets or components of the cell cycle machinery. Rather, major differences are detected in genes associated with cell migration, survival and differentiation.

Our approach differs from several recent studies of gene expression analysis in medulloblastoma (Boon et al., 2003; Kho et al., 2004; Lee et al., 2003; MacDonald et al., 2001; Park et al., 2003; Pomeroy et al., 2002; Wechsler-Reya, 2003). In most cases, these investigators compared medulloblastoma with other brain tumors or with normal adult cerebellum. For example, Pomeroy et al. found that medulloblastoma has a distinct gene expression profile compared with other pediatric brain tumors (Pomeroy et al., 2002). In particular, desmoplastic medulloblastomas (which often harbor mutations in the hedgehog pathway) have elevated expression of hedgehog target genes such as *Nmyc*, *patched*, *gli1* and *IGF2* (insulin-like growth factor 2). Similarly, Boon et al. used serial analysis of gene expression (SAGE) to compare human medulloblastoma and normal brain, and found increased expression of hedgehog targets and cell cycle regulators such as Nmyc and thymidylate synthase (Boon et al., 2003; Oliver et al., 2003). These findings are consistent with the fact that medulloblastoma cells are highly proliferative cells that exhibit hedgehog pathway activation, whereas normal brain consists primarily of post-mitotic neurons in which the hedgehog pathway is inactive. In contrast to these studies, we compared medulloblastoma cells with their cells of origin, proliferating GCPs. This allowed us to control for proliferation and hedgehog pathway activation and, instead, to identify other genes that may play an important role in tumor progression.

Similar to our studies, Lee et al. analyzed gene expression in medulloblastoma and in neonatal cerebellum (Lee et al., 2003). Both studies found that gene expression in medulloblastoma was much more similar to neonatal cerebellum than to adult cerebellum. Yet there were also key differences between these studies. In particular, Lee et al. found that medulloblastoma is characterized by increased expression of genes associated with the granule cell lineage, hedgehog pathway activation and proliferation (*math1*, *srebp*, *hexokinase*, *Nmyc*, *cyclin D1*, *sfrp1*), whereas we did not detect elevated expression of these genes. One important distinction between the two studies is the use of intact tissues versus dissociated cells. Lee et al. compared intact tumor tissue (which consists largely of GCP-like cells) and intact neonatal cerebellum (which contains not only GCPs but also significant numbers of post-mitotic granule cells and other cell types). By contrast, we compared purified populations of GCPs, pre-neoplastic cells and tumor cells, all of which are highly enriched for proliferating GCP-like cells. As a result, genes associated with cell lineage and degree of hedgehog pathway activity were not differentially expressed in our screen.

Dysregulation of migration, differentiation and apoptosis in medulloblastoma

Our study is unique in that we compared gene expression in similar populations of cells at three different stages of tumor progression. This allowed us to identify genes that distinguish these stages. Interestingly, many of these genes were regulators of migration, survival and differentiation, processes that have been studied in the context of normal granule cell development but were not previously known to play a role in medulloblastoma. Most prominent among these genes were regulators of cell migration. These included transcription factors (Pax6), surface receptors (Unc5h3), secreted proteins (PAF acetylhydrolase) and ECM molecules (Collagen) that have been implicated in granule cell migration (Engelkamp et al., 1999; Fishman and Hatten, 1993; Przyborski et al., 1998; Tokuoka et al., 2003). Notably, the majority of the genes we identified have been found to promote migration, and were downregulated in pre-neoplastic cells. Decreased expression of these genes during the early stages of tumorigenesis is interesting because pre-neoplastic cells clearly exhibit aberrant migration: whereas GCPs migrate inward during normal development, pre-neoplastic cells (and tumor cells) remain stuck on the surface of the cerebellum. A similar location has been noted for human medulloblastomas, which often spread through the meninges but rarely invade the inner layers of the cerebellum (Koeller and Rushing, 2003).

It has long been unclear how failure to migrate inward is related to tumorigenesis. One possibility is that pre-neoplastic cells and tumor cells are unable to migrate because they are proliferating or locked in a precursor state. Alternatively, the inability to migrate could be an intrinsic defect that plays an essential role in tumorigenesis. For example, by losing the ability to migrate, cells may remain trapped in an environment (e.g. close to the pial surface) that facilitates their continued growth and survival. Our finding that genes involved in migration are downregulated in pre-neoplastic cells strongly supports the notion of an intrinsic defect. However, further experiments will be necessary to determine whether changes in migration-associated genes are necessary for the development of medulloblastoma.

Genes that regulate differentiation may also be crucial in determining the course of tumorigenesis. Importantly, we found that pre-neoplastic cells have reduced expression of genes associated with granule cell differentiation (e.g. Zic3 and Neurod1). This is consistent with the fact that these cells continue to proliferate and retain expression of GCP markers, whereas normal GCPs can exit the cell cycle and differentiate into mature granule neurons. Whether the inability to differentiate is a cause or a consequence of transformation remains to be determined, but the identification of specific transcription factors that may regulate this process will allow us to test the significance of differentiation directly. Further studies perturbing the expression of these factors in vivo are underway.

Finally, our data suggest that altered stress responses may contribute to tumor formation in *patched* mutant mice. Heat-shock proteins, co-chaperones (Hsp60, Hsp105, Dnajb1, Dnajb10 and Bag3) and the transcription factor Atf3 all function to protect cells from stress-induced apoptosis and necrosis (Hatayama et al., 2001; Nakagomi et al., 2003; Takayama et al., 2003). The increased expression of these genes in pre-neoplastic cells and tumor cells may reflect an increased ability to survive under stress conditions, which may be crucial for the early stages of tumorigenesis. In fact, several lines of evidence suggest that dysregulation of apoptosis or stress responses may be important for medulloblastoma formation. For example, crossing *patched* mutant mice with homozygous p53 knockout mice leads to a dramatic increase in tumor incidence: whereas only 14-20% of *patched* heterozygotes develop medulloblastoma, more than 95% of $patched^{+/-}/p53^{-/-}$ mice develop tumors (Wetmore et al., 2001). Similarly, animals that lack both p53 and PARP1, an enzyme that promotes cell death in response to DNA damage, develop medulloblastoma (Tong et al., 2003). Notably, no mutations in p53 have been found in tumors from *patched* heterozygotes (Wetmore et al., 2001), suggesting that in these animals some other element of the apoptotic machinery may need to be inactivated for tumors to form. The genes we have found to be upregulated in pre-neoplastic cells may provide some important clues to the mechanisms by which apoptosis is subverted in medulloblastoma.

The identification of a pre-neoplastic stage in murine medulloblastoma raises the possibility that a similar stage exists in the human disease. If so, the genes we have identified as markers of pre-neoplastic cells may be useful for early detection of medulloblastoma, particularly in people with an inherited susceptibility to the disease (Gorlin, 1987; Hamilton et al., 1995). Detection of medulloblastoma at early stages may increase the effectiveness of conventional medulloblastoma therapy. In addition, if the genes we have identified play a causal role in tumor progression, they may serve as valuable targets for therapy. Recent studies suggest that pharmacologic antagonists of the hedgehog pathway may be effective at inhibiting growth of medulloblastoma cells in vitro and in vivo (Berman et al., 2002; Romer et al., 2004). Therefore, identification of other pathways that are crucial for tumorigenesis may open up new avenues for treatment of this devastating disease.

We thank Holly Dressman, Laura Reid, and the Duke Microarray Core Facility for microarray processing, Mike Cook and Lynn Martinek for flow cytometric analysis, and Thomas Cummings for interpretation of histological staining. We are also grateful to Wieland Huttner and Denis Corbeil for anti-prominin/CD133 antibodies, to Jane Johnson for Math1-GFP mice, to Audra Carroll for helpful discussions, and to Terry Van Dyke, Phil Beachy and Chris Counter for critical review of the manuscript. T.G.O. is a National Science Foundation graduate student fellow and R.J.W.-R. is a Kimmel Foundation Scholar. This research was supported by a McDonnell Foundation 21st Century Award and by funds from the Children's Brain Tumor Foundation.

Supplementary material

Supplementary material for this article is available at
http://dev.biologists.org/cgi/content/full/132/10/2425/DC1

References

Adams, N. C., Tomoda, T., Cooper, M., Dietz, G. and Hatten, M. E. (2002). Mice that lack astrotactin have slowed neuronal migration. *Development* **129**, 965-972.

Ben-Arie, N., McCall, A. E., Berkman, S., Eichele, G., Bellen, H. J. and Zoghbi, H. Y. (1996). Evolutionary conservation of sequence and

expression of the bHLH protein Atonal suggests a conserved role in neurogenesis. *Hum. Mol. Genet.* **5**, 1207-1216.
Benjamini, Y. and Hochberg, Y. (1995). Controlling the false discovery rate: a practical and powerful approach to multiple testing. *J. R. Stat. Soc. B* **57**, 289-300.
Berman, D. M., Karhadkar, S. S., Hallahan, A. R., Pritchard, J. I., Eberhart, C. G., Watkins, D. N., Chen, J. K., Cooper, M. K., Taipale, J., Olson, J. M. et al. (2002). Medulloblastoma growth inhibition by hedgehog pathway blockade. *Science* **297**, 1559-1561.
Bignami, A., Eng, L. F., Dahl, D. and Uyeda, C. T. (1972). Localization of the glial fibrillary acidic protein in astrocytes by immunofluorescence. *Brain Res.* **43**, 429-435.
Boon, K., Edwards, J. B., Siu, I. M., Olschner, D., Eberhart, C. G., Marra, M. A., Strausberg, R. L. and Riggins, G. J. (2003). Comparison of medulloblastoma and normal neural transcriptomes identifies a restricted set of activated genes. *Oncogene* **22**, 7687-7694.
Borghesani, P. R., Peyrin, J. M., Klein, R., Rubin, J., Carter, A. R., Schwartz, P. M., Luster, A., Corfas, G. and Segal, R. A. (2002). BDNF stimulates migration of cerebellar granule cells. *Development* **129**, 1435-1442.
Buhren, J., Christoph, A. H., Buslei, R., Albrecht, S., Wiestler, O. D. and Pietsch, T. (2000). Expression of the neurotrophin receptor p75NTR in medulloblastomas is correlated with distinct histological and clinical features: evidence for a medulloblastoma subtype derived from the external granule cell layer. *J. Neuropathol. Exp. Neurol.* **59**, 229-240.
Corcoran, R. B. and Scott, M. P. (2001). A mouse model for medulloblastoma and basal cell nevus syndrome. *J. Neurooncol.* **53**, 307-318.
Dalgaard, P. (2002). Introductory statistics with R. New York: Springer Verlag.
Eisen, M. B., Spellman, P. T., Brown, P. O. and Botstein, D. (1998). Cluster analysis and display of genome-wide expression patterns. *Proc. Natl. Acad. Sci. USA* **95**, 14863-14868.
Ellison, D. W., Clifford, S. C., Gajjar, A. and Gilbertson, R. J. (2003). What's new in neuro-oncology? Recent advances in medulloblastoma. *Eur. J. Pediatr. Neurol.* **7**, 53-66.
Engelkamp, D., Rashbass, P., Seawright, A. and van Heyningen, V. (1999). Role of Pax6 in development of the cerebellar system. *Development* **126**, 3585-3596.
Faust, P. L. (2003). Abnormal cerebellar histogenesis in PEX2 Zellweger mice reflects multiple neuronal defects induced by peroxisome deficiency. *J. Comp. Neurol.* **461**, 394-413.
Fishman, R. B. and Hatten, M. E. (1993). Multiple receptor systems promote CNS neural migration. *J. Neurosci.* **13**, 3485-3495.
Gentleman, R. and Carey, V. (2002). Bioconductor. *R. News* **2**, 11-16.
Goodrich, L. V., Johnson, R. L., Milenkovic, L., McMahon, J. A. and Scott, M. P. (1996). Conservation of the hedgehog/patched signaling pathway from flies to mice: induction of a mouse patched gene by Hedgehog. *Genes Dev.* **10**, 301-312.
Goodrich, L. V., Milenkovic, L., Higgins, K. M. and Scott, M. P. (1997). Altered neural cell fates and medulloblastoma in mouse *patched* mutants. *Science* **277**, 1109-1113.
Gorlin, R. J. (1987). Nevoid basal-cell carcinoma syndrome. *Medicine* **66**, 98-113.
Hahn, H., Wicking, C., Zaphiropoulous, P. G., Gailani, M. R., Shanley, S., Chidambaram, A., Vorechovsky, I., Holmberg, E., Unden, A. B., Gillies, S. et al. (1996). Mutations of the human homolog of Drosophila patched in the nevoid basal cell carcinoma syndrome. *Cell* **85**, 841-851.
Hahn, H., Wojnowski, L., Specht, K., Kappler, R., Calzada-Wack, J., Potter, D., Zimmer, A., Muller, U., Samson, E. and Quintanilla-Martinez, L. (2000). Patched target Igf2 is indispensable for the formation of medulloblastoma and rhabdomyosarcoma. *J. Biol. Chem.* **275**, 28341-28344.
Hamilton, S. R., Liu, B., Parsons, R. E., Papadopoulos, N., Jen, J., Powell, S. M., Krush, A. J., Berk, T., Cohen, Z., Tetu, B. et al. (1995). The molecular basis of Turcot's syndrome. *New Engl. J. Med.* **332**, 839-347.
Hatayama, T., Yamagishi, N., Minobe, E. and Sakai, K. (2001). Role of hsp105 in protection against stress-induced apoptosis in neuronal PC12 cells. *Biochem. Biophys. Res. Commun.* **288**, 528-534.
Helms, A. W. and Johnson, J. E. (1998). Progenitors of dorsal commissural interneurons are defined by MATH1 expression. *Development* **125**, 919-928.
Hemmati, H. D., Nakano, I., Lazareff, J. A., Masterman-Smith, M., Geschwind, D. H., Bronner-Fraser, M. and Kornblum, H. I. (2003). Cancerous stem cells can arise from pediatric brain tumors. *Proc. Natl. Acad. Sci. USA* **100**, 15178-15183.
Ingham, P. W. and McMahon, A. P. (2001). Hedgehog signaling in animal development: paradigms and principles. *Genes Dev.* **15**, 3059-3087.
Johnson, R. L., Rothman, A. L., Xie, J., Goodrich, L. V., Bare, J. W., Bonifas, J. M., Quinn, A. G., Myers, R. M., Cox, D. R., Epstein, E. H., Jr et al. (1996). Human homolog of patched, a candidate gene for the basal cell nevus syndrome. *Science* **272**, 1668-1671.
Kadin, M. E., Rubinstein, L. J. and Nelson, J. S. (1970). Neonatal cerebellar medulloblastoma originating from the fetal external granular layer. *J. Neuropathol. Exp. Neurol.* **29**, 583-600.
Kenney, A. M. and Rowitch, D. H. (2000). Sonic hedgehog promotes G(1) cyclin expression and sustained cell cycle progression in mammalian neuronal precursors. *Mol. Cell. Biol.* **20**, 9055-9067.
Kenney, A. M., Cole, M. D. and Rowitch, D. H. (2003). Nmyc upregulation by sonic hedgehog signaling promotes proliferation in developing cerebellar granule neuron precursors. *Development* **130**, 15-28.
Kho, A. T., Zhao, Q., Cai, Z., Butte, A. J., Kim, J. Y., Pomeroy, S. L., Rowitch, D. H. and Kohane, I. S. (2004). Conserved mechanisms across development and tumorigenesis revealed by a mouse development perspective of human cancers. *Genes Dev.* **18**, 629-440.
Kim, J. Y., Nelson, A. L., Algon, S. A., Graves, O., Sturla, L. M., Goumnerova, L. C., Rowitch, D. H., Segal, R. A. and Pomeroy, S. L. (2003). Medulloblastoma tumorigenesis diverges from cerebellar granule cell differentiation in patched heterozygous mice. *Dev. Biol.* **263**, 50-66.
Koeller, K. K. and Rushing, E. J. (2003). From the archives of the AFIP: medulloblastoma: a comprehensive review with radiologic-pathologic correlation. *Radiographics* **23**, 1613-1637.
Lam, C. W., Xie, J., To, K. F., Ng, H. K., Lee, K. C., Yuen, N. W., Lim, P. L., Chan, L. Y., Tong, S. F. and McCormick, F. (1999). A frequent activated smoothened mutation in sporadic basal cell carcinomas. *Oncogene* **18**, 833-836.
Lee, Y., Miller, H. L., Jensen, P., Hernan, R., Connelly, M., Wetmore, C., Zindy, F., Roussel, M. F., Curran, T., Gilbertson, R. J. et al. (2003). A molecular fingerprint for medulloblastoma. *Cancer Res.* **63**, 5428-5437.
Lumpkin, E. A., Collisson, T., Parab, P., Omer-Abdalla, A., Haeberle, H., Chen, P., Doetzlhofer, A., White, P., Groves, A., Segil, N. et al. (2003). Math1-driven GFP expression in the developing nervous system of transgenic mice. *Gene Expr. Patterns* **3**, 389-395.
MacDonald, T. J., Brown, K. M., LaFleur, B., Peterson, K., Lawlor, C., Chen, Y., Packer, R. J., Cogen, P. and Stephan, D. A. (2001). Expression profiling of medulloblastoma: PDGFRA and the RAS/MAPK pathway as therapeutic targets for metastatic disease. *Nat. Genet.* **29**, 143-152.
Messer, A. and Hatch, K. (1984). Persistence of cerebellar thymidine kinase in staggerer and hypothyroid mutants. *J. Neurogenet.* **1**, 239-248.
Miyata, H., Ikawa, E. and Ohama, E. (1998). Medulloblastoma in an adult suggestive of external granule cells as its origin: a histological and immunohistochemical study. *Brain Pathol.* **15**, 31-35.
Nakagomi, S., Suzuki, Y., Namikawa, K., Kiryu-Seo, S. and Kiyama, H. (2003). Expression of the activating transcription factor 3 prevents c-Jun N-terminal kinase-induced neuronal death by promoting heat shock protein 27 expression and Akt activation. *J. Neurosci.* **23**, 5187-5196.
Oliver, T. G. and Wechsler-Reya, R. J. (2004). Getting at the root and stem of brain tumors. *Neuron* **42**, 885-888.
Oliver, T. G., Grasfeder, L. L., Carroll, A. L., Kaiser, C., Gillingham, C. L., Lin, S. M., Wickramasinghe, R., Scott, M. P. and Wechsler-Reya, R. J. (2003). Transcriptional profiling of the Sonic hedgehog response: a critical role for N-myc in proliferation of neuronal precursors. *Proc. Natl. Acad. Sci. USA* **100**, 7331-7336.
Park, P. C., Taylor, M. D., Mainprize, T. G., Becker, L. E., Ho, M., Dura, W. T., Squire, J. and Rutka, J. T. (2003). Transcriptional profiling of medulloblastoma in children. *J. Neurosurg.* **99**, 534-541.
Pomeroy, S. L., Tamayo, P., Gaasenbeek, M., Sturla, L. M., Angelo, M., McLaughlin, M. E., Kim, J. Y., Goumnerova, L. C., Black, P. M., Lau, C. et al. (2002). Prediction of central nervous system embryonal tumour outcome based on gene expression. *Nature* **415**, 436-442.
Przyborski, S. A., Knowles, B. B. and Ackerman, S. L. (1998). Embryonic phenotype of Unc5h3 mutant mice suggests chemorepulsion during the formation of the rostral cerebellar boundary. *Development* **125**, 41-50.
Raffel, C., Jenkins, R. B., Frederick, L., Hebrink, D., Alderete, B., Fults, D. W. and James, C. D. (1997). Sporadic medulloblastomas contain PTCH mutations. *Cancer Res.* **57**, 842-845.
Romer, J. T., Kimura, H., Magdaleno, S., Sasai, K., Fuller, C., Baines, H., Connelly, M., Stewart, C. F., Gould, S., Rubin, L. L. et al. (2004).

Suppression of the Shh pathway using a small molecule inhibitor eliminates medulloblastoma in Ptc1(+/–)p53(–/–) mice. *Cancer Cell* **6**, 229-240.

Sawamoto, K., Nakao, N., Kakishita, K., Ogawa, Y., Toyama, Y., Yamamoto, A., Yamaguchi, M., Mori, K., Goldman, S. A., Itakura, T. et al. (2001). Generation of dopaminergic neurons in the adult brain from mesencephalic precursor cells labeled with a nestin-GFP transgene. *J. Neurosci.* **21**, 3895-3903.

Singh, S. K., Clarke, I. D., Terasaki, M., Bonn, V. E., Hawkins, C., Squire, J. and Dirks, P. B. (2003). Identification of a cancer stem cell in human brain tumors. *Cancer Res.* **63**, 5821-5828.

Singh, S. K., Clarke, I. D., Hide, T. and Dirks, P. B. (2004). Cancer stem cells in nervous system tumors. *Oncogene* **23**, 7267-7273.

Sommer, I. and Schachner, M. (1981). Monoclonal antibodies (O1 to O4) to oligodendrocyte surfaces: An immunocytological study in the central nervous system. *Dev. Biol.* **83**, 311-327.

Takayama, S., Reed, J. C. and Homma, S. (2003). Heat-shock proteins as regulators of apoptosis. *Oncogene* **22**, 9041-9047.

Taylor, M. D., Liu, L., Raffel, C., Hui, C. C., Mainprize, T. G., Zhang, X., Agatep, R., Chiappa, S., Gao, L., Lowrance, A. et al. (2002). Mutations in SUFU predispose to medulloblastoma. *Nat. Genet.* **31**, 306-310.

Tokuoka, S. M., Ishii, S., Kawamura, N., Satoh, M., Shimada, A., Sasaki, S., Hirotsune, S., Wynshaw-Boris, A. and Shimizu, T. (2003). Involvement of platelet-activating factor and LIS1 in neuronal migration. *Eur. J. Neurosci.* **18**, 563-570.

Tong, W. M., Ohgaki, H., Huang, H., Granier, C., Kleihues, P. and Wang, Z. Q. (2003). Null mutation of DNA strand break-binding molecule poly(ADP-ribose) polymerase causes medulloblastomas in p53(–/–) mice. *Am. J. Pathol.* **162**, 343-352.

Traiffort, E., Charytoniuk, D., Watroba, L., Faure, H., Sales, N. and Ruat, M. (1999). Discrete localizations of hedgehog signalling components in the developing and adult rat nervous system. *Eur. J. Neurosci.* **11**, 3199-3214.

Vaillant, C., Meissirel, C., Mutin, M., Belin, M. F., Lund, L. R. and Thomasset, N. (2003). MMP-9 deficiency affects axonal outgrowth, migration, and apoptosis in the developing cerebellum. *Mol. Cell. Neurosci.* **24**, 395-408.

Wechsler-Reya, R. J. (2003). Analysis of Gene Expression in the Normal and Malignant Cerebellum. *Recent Prog. Horm. Res.* **58**, 249-261.

Wechsler-Reya, R. J. and Scott, M. P. (1999). Control of neuronal precursor proliferation in the cerebellum by Sonic Hedgehog. *Neuron* **22**, 103-114.

Wechsler-Reya, R. and Scott, M. P. (2001). The developmental biology of brain tumors. *Annu. Rev. Neurosci.* **24**, 385-428.

Weigmann, A., Corbeil, D., Hellwig, A. and Huttner, W. B. (1997). Prominin, a novel microvilli-specific polytopic membrane protein of the apical surface of epithelial cells, is targeted to plasmalemmal protrusions of non-epithelial cells. *Proc. Natl. Acad. Sci. USA* **94**, 12425-12430.

Wetmore, C., Eberhart, D. E. and Curran, T. (2000). The normal patched allele is expressed in medulloblastomas from mice with heterozygous germ-line mutation of patched. *Cancer Res.* **60**, 2239-2246.

Wetmore, C., Eberhart, D. E. and Curran, T. (2001). Loss of p53 but not ARF accelerates medulloblastoma in mice heterozygous for patched. *Cancer Res.* **61**, 513-516.

Yokota, N., Aruga, J., Takai, S., Yamada, K., Hamazaki, M., Iwase, T., Sugimura, H. and Mikoshiba, K. (1996). Predominant expression of human zic in cerebellar granule cell lineage and medulloblastoma. *Cancer Res.* **56**, 377-383.

Zakhary, R., Keles, G. E., Aldape, K. and Berger, M. S. (2001). Medulloblastoma and primitive neuroectodermal tumors. In *Brain Tumors: An Encyclopedic Approach* (ed. A. H. Kaye and E. R. Law), pp. 605-615. London: Churchill Livingstone.

Zurawel, R. H., Allen, C., Wechsler-Reya, R., Scott, M. P. and Raffel, C. (2000). Evidence that haploinsufficiency of Ptch leads to medulloblastoma in mice. *Genes Chromosomes Cancer* **28**, 77-81.

Table S1. Phenotype of GCPs, pre-neoplastic cells and tumor cells from *patched* mutant mice

	GCP	Pre-neoplastic	Tumor
Math-1 (GFP)	91	87	95
Psa-Ncam	68	31	80
Zic-1	90	35	77
TUJ1	10	77	39
A2B5	79	85	85
O4	2	15	7
GFAP	4	4	4
Nestin	2	2	3
CD133	2	0	0

Cells were isolated and either stained with antibodies against surface markers (CD133/prominin, O4, PSA-NCAM, A2B5) and analyzed by flow cytometry, or allowed to adhere to coverslips and stained with antibodies to intracellular markers (TuJ1, NeuN, Math1, Zic1, Nestin, GFAP) and analyzed by immunofluorescence microscopy. Numbers indicate the percentage of positive cells determined by flow cytometry or by counting and averaging 3-4 fields from three independent samples of each cell type.